STUDYING HEAT TRANSFER AND FLUID FLOW DISTRIBUTION ON HEATED FIN INSIDE RECTANGULAR DUCT WITH USING TRIANGULAR PROTRUSION

Dr. Ahmed Hashm Yousif
Mechanical Department
AL-Diwania Technical Institute

Abas Naji
Mechanical Department
AL-Diwania Technical Institute

Dr. Kareem Dakeel Jasem
Mechanical Department
AL-Diwania Technical Institute

Abstract

The structure of flow and heat transfer characteristics over a heated fin (at constant heat flux) in rectangular duct with using triangle protrusion has been studied numerically. An incompressible flow and finite volumes method (FVM) in general coordinates with collocated grid arrangement are used to solve two dimensions continuity, Navier – Stokes and energy equations. The Prandtl number and Reynolds number are takes as 0.71 and 2000 respectively.

At present study, different lengths of base of triangle protrusion (d/H = 0, 0.26, 0.53, 0.8, 1.07, 1.33) at (l/H= 0.13) was used. The results were compared with the case of flow inside duct without using protrusion. The results indicate that heat transfer and pressure drop is affected by the length of protrusion base especially near the triangle protrusion. The results illustrate that the heat transfer will be increasing with decreases the length of protrusion base. This study identifies an enhancement in the average heat transfer with increasing in pressure drop.

دراسة انتقال الحرارة وجريان الموائع على زعنفة ساخنة داخل مجرى مستطيل بوجود نتوء مثلثي الشكل

د. احمد هاشم يوسف
قسم الميكانيك
المعهد التقني – الديوانية

عباس ناجي خضير
قسم الميكانيك
المعهد التقني – الديوانية

د. كريم داخل جاسم
قسم الميكانيك
المعهد التقني – الديوانية

الخلاصة

أجريت دراسة عددية لمعرفة خواص انتقال الحرارة والجريان على زعنفة ساخنة داخل مجرى مستطيل المقطع(بفيض حراري ثابت) بوجود نتوء مثلثي الشكل. تم أستخدم طريقة الحجوم المحددة(FVM) لجريان لا انضغاطي، وتم استخدام ترتيب الشبكة غير المتناوبةcollocated grid لحل معادلات نافير – ستوك، الكتلة والطاقة ثنائية البعد. وقد تم أخذ رقم برانتل0.71 ورقم رينولدز2000.

تمت دراسة تأثير طول قاعدة النتوء (d/H = 0, 0.26, 0.53, 0.8, 1.07, 1.33)على الهبوط بالضغط وانتقال الحرارة على الصفيحة داخل المجرى حيث إن(H) يمثل ارتفاع المجرى. تم مقارنة النتائج مع حالة الجريان بدون استخدام نتوء. أوضحت النتائج أن لهذا النتوء اثر كبير على الهبوط بالضغط وانتقال الحرارة على الصفيحة وخصوصا" قرب النتوء. بينت هذه الدراسة أن معدل انتقال الحرارة يتحسن بوجود النتوء مع زيادة بهبوط الضغط.

Nomenclature

Symbol	Description	Unit
A	Convection-diffusion discritization coefficient	
a_1, a_2	Transformation coefficients	
B	Channel length	m
C_p	Static pressure coefficient	
d	Length of protrusion base	m
D	Diffusion term coefficient	
F	Mass flux	
H	Channel height	m
h_{ij}	Local heat transfer coefficient	$W/(m^2.K)$
J	Jacobean of transformation	m
k	Thermal conductivity	W/(m.k)
l	Triangle protrusion height	
Nu	Nusselt number	
P	Source term in grid generation system of equation	
	pressure	N/m^2
P_0	Total pressure	N/m^2
P_{ij}	Local static pressure	N/m^2
P_r	Prandtl number	
q	Heat flux per unit area	W/m^2
Q	Source term in grid generation system of equation	
Re	Reynolds number	
S	Source term for the dependent variable Φ	
T	Temperature	K
u	Velocity in x-direction	m/s
U, V	Contravariant velocities	
v	Velocity in y- direction	m/s
x, y	Cartesian coordinates	

Greek Symbols

Symbol	Description	Unit
ξ, η	General coordinates	
Φ	General variable	
α	Thermal diffusivity	
μ	Kinetic viscosity	Kg/m^3
ρ	Density	Kg/m^3
Γ	Coefficient of Diffusivity	

Abbreviation

Symbol	Description	Unit
2-D	Two dimensions	
FVM	Finite volume method	
N-S	Naveir-Stoke equation	
PDE	Partial differential equation	

Subscripts

Symbol	Description	Unit
b	Bulk	
e,w,n,s	Face of control volume	
E,W,N,S	Neighbor nodes of node (P)	
f	Fluid	
p	Center of control volume	
ij	Index control in (x,y) or (ξ, η) direction	
in	Inlet condition	
Φ	Total source of Φ transport property	
w	wall	

Introduction

Compact heat exchangers are widely employed in engineering application, especially in automotive industry, air conditioning and refrigeration apparatus (Ahmed 2003). The improvement in design of these heat exchangers has attracted many researchers.

The heat transfer coefficients on the flat surface are significantly law due to increase the boundary layer thickness and in order to increase the heat transfer between the gas and fin in plat fin heat exchanger, protrusions can be used on the flat surface (Isak,1998). Many researchers used different types of vortex generators to generate a longitudinal vortex to mixing the fluid near the wall with main fluid that lead to remove heat near the wall to the main flow.

In plate – fin or tube heat exchangers the flow between the plates can be considered as a duct flow. To reduction the thermal resistance, the heat transfer coefficient need to be augmented (Tiggelbeek,1991).

In plate – fin heat exchanger, the heat transfer coefficient is significantly law and in order to increase heat transfer between the fluid and plates, protrusions or vortex generators can be use and fluid flow and heat transfer on flat plates with using vortex generators was experimentally and numerically investigated. The researchers (Ahmed 2003), (Biswas, 1992) and (Fiebig, 1989) are investigated flow and heat transfer on flat – plate with using wing and winglet type vortex that the heat transfer enhanced by using vortex generators with increasing in pressure drop across the plates. The studies of (Tiggelbeek, 1991), (Isak,1998) and (Russell, 1982) investigated the flow and heat transfer from plates with using obstacles and vortex generators experimentally. The studies show that heat transfer enhanced with using obstacles and vortex generator. One relevant application using such flow configuration is the heat transfer between the flow and plates in the case of plate - fin heat exchangers,as shown in **Figure (1)** (Isak,1998).

In the present paper, a numerical investigation is described to study forced convection heat transfer with using single triangle protrusion in a rectangular channel as a part of plate – fin heat exchanger with different ratio d/H = (0 , 0.26 ,0.53 ,0.8 ,1.07 ,1.33 ,) at (l/H =0.13) as showing in **Figure (2)** for Re=2000 and pr=0.71.

The local heat transfer in front region of plate is relatively high and decreases toward the rear due to growth of boundary layer, therefore the strategy of this study is to place a triangle protrusion in the middle of channel to mixing the fluid near the wall with the main fluid and to increase the velocity of flow near the protrusion to sweep the hot area or to make a vortex in the flow.

Mathematical Model

The mathematical analysis is presented for partial differential equation (PDE) which describe fully developing flow and heat transfer at Re=2000 in parallel plate channel. Incompressible flow and steady state is assembly in entrance region with neglecting body force, heat conduction and free convection.

Grid Generation

Figure (3) show the schematic of two dimensions body fitting grid used for present computation, this grid obtained by solving non homogeneous 2-D Laplace equations (Thompson, 1977).

$$\xi_{xx}+\xi_{yy}=P(\xi,\eta)$$
$$\eta_{xx}+\eta_{yy}=Q(\xi,\eta) \qquad (1)$$

Where P and Q are used to cluster the grid near the wall to sense the velocity gradient because there is a friction between the wall and the fluid. Equations (1) are transformed to (ξ, η) coordinates by interchanging the roles of dependent variables. This yields the following system equations.

$$\left.\begin{aligned} g_{11}x_{\xi\xi}-g_{21}x_{\xi\eta}+g_{22}x_{\eta\eta}&=-J^2(Px_\xi+Qx_\eta)\\ g_{11}y_{\xi\xi}-g_{21}y_{\xi\eta}+g_{22}y_{\eta\eta}&=-J^2(Py_\xi+Qy_\eta)\end{aligned}\right\} \qquad (2)$$

Where

$g_{11}=x_\eta^2+y_\eta^2$
$g_{21}=2(x_\xi x_\eta+y_\xi y_\eta)$
$g_{22}=x_\xi^2+y_\xi^2$
$J=x_\xi y_\eta-x_\eta y_\xi$

Because the geometry of the domain was complex the (2-D) N-S, continuity and energy equations must be transported to general coordinates (ξ, η). Physical and Computational Plane with collocated grid arrangement can be seen in **Figure (4).**

Governing Equations

The 2-D governing equations of mass, momentum and energy equations for steady incompressible flow can be written as follows:-
Continuity equation

$$\frac{\partial u}{\partial x}+\frac{\partial v}{\partial y}=0 \qquad (3)$$

Momentum equation

$$u\frac{\partial u}{\partial x}+v\frac{\partial u}{\partial y}=-\frac{1}{\rho}\frac{\partial p}{\partial x}+v\frac{\partial^2 u}{\partial y^2}$$
$$u\frac{\partial v}{\partial x}+v\frac{\partial v}{\partial y}=-\frac{1}{\rho}\frac{\partial p}{\partial y}+u\frac{\partial^2 v}{\partial x^2} \qquad (4)$$

Energy equation

$$u\frac{\partial T}{\partial x}+v\frac{\partial T}{\partial y}=\alpha\frac{\partial^2 T}{\partial y^2} \qquad (5)$$

The above equations can be written in a general transport equation as :-

$$\frac{\partial(\rho u\phi)}{\partial x}+\frac{\partial(\rho v\phi)}{\partial y}=\frac{\partial}{\partial x}\left[\Gamma_\phi(\frac{\partial\phi}{\partial x})\right]+\frac{\partial}{\partial y}\left[\Gamma_\phi(\frac{\partial\phi}{\partial y})\right]+S_\phi \qquad (6)$$

This equation serves as a starting point for computational procedure in (FVM), by setting (Φ=1, Γ_Φ=0 and S_Φ=0) the continuity equation can be obtain, by setting (Φ=u, v and $\Gamma_\Phi=\mu$), N-S equation can be obtain and by setting (Φ=T and $\Gamma_\Phi=\mu/pr$) the energy equation can be obtain. The two terms in the left of the general transport equation (6) are convective terms, the first two terms in the right side of general transport equation (6) are diffusive terms and the last term is the source term.

For the general curvilinear coordinates system (ξ, η), the general transport equation (6) can be transformed to the following form:-

$$\frac{\partial}{\partial\xi}(\rho U\Phi-\frac{a1\Gamma_\Phi}{J}\frac{\partial\Phi}{\partial\xi})+\frac{\partial}{\partial\eta}(\rho V\Phi-\frac{a2\Gamma_\Phi}{J}\frac{\partial\Phi}{\partial\eta})=S_{NEW} \qquad (7)$$

where (U, V) are the contravariant velocity components as shown in **Figure (5).**

And S_{NEW} =JS+S_N where S_N is the source term due to non orthogonal characteristic of grid system which disappear under orthogonal grid system.

The transformation coefficients (a_1, a_2)are defined as:-

$$a1=\xi_x^2+\xi_y^2$$
$$a2=\eta_x^2+\eta_y^2 \qquad (8)$$

And the transformation metrics are calculated as follows

$$\left.\begin{aligned}\xi_x&=\frac{y_\xi}{J}\\ \xi_y&=\frac{-x_\eta}{J}\\ \eta_x&=\frac{-y_\xi}{J}\\ \eta_y&=\frac{x_\xi}{J}\end{aligned}\right\} \qquad (9)$$

For collocated grid arrangement, all properties must be at the center of control volume (P) as shown in **Figure (4).** And the integration of equation (7) over control volume gives

$$[(\rho U\Phi)-(\frac{a1\Gamma_{\Phi}\Phi_{\xi}}{J})\Delta\eta]_{w}^{e}+[(\rho V\Phi)-(\frac{a2\Gamma_{\Phi}\Phi_{\eta}}{J})\Delta\xi]_{s}^{n}=dvS_{NEW} \qquad (10)$$

Where $dv=\Delta\xi\,\Delta\eta$

To interpolate convection and diffusion terms, the power law difference scheme (Patenker, 1980)can be used, and the following algebraic equation can be obtained:-

$$A_p\Phi_p = A_E\Phi_E + A_W\Phi_W + A_N\Phi_N + A_S\Phi_S + dv\, S_{NEW} \qquad (11)$$

Where

$A_E= D_e*A(|P_{\Delta e}|)+[[-F_e, 0]]$

$A_W=D_w*A(|P_{\Delta w}|)+[[F_w, 0]]$

$A_N= D_n*A(|P_{\Delta n}|)+[[-F_n, 0]]$

$A_S= Ds*A(|P_{\Delta s}|)+[[F_s, 0]]$

$A_p= A_E+ A_W+ A_N+ A_S$

when (F) is the mass flux and (D) is the diffusion term coefficient

In order to avoid the checkerboard pressure field in collocated grid system, a momentum interpolation technique on cell face was successfully proposed by Rhie and Chow interpolation method that developed by (Ferzigen, 1999).

Boundary Conditions

The (FVM) required that the boundary flux, either be known or expressed in term of known quantities on interior nodal value. the boundary of the present work include solid wall, inlet and outlet planes.

1 Inlet boundary

Usually at inlet boundary, all quantities have to be prescribed as follows:-

$$\left.\begin{array}{l}(u)_{inlet}=u_{in}\\(v)_{inlet}=v_{in}\\(p)_{inlet}=p_{in}\\(T)_{inlet}=T_{in}\end{array}\right\} \qquad (12)$$

2 Outlet boundary

Always all values of dependent variables are unknown at exit boundary. It is often adequate to set outlet boundary values equal to intermediate up stream neighbor (e.g $\Phi_E= \Phi_p$). This is equivalent to saying the first derivative of property Φ in the direction normal to the boundary is equal to zero.

$$\left.\begin{array}{l}\frac{\partial u}{\partial x}=0\\\frac{\partial v}{\partial x}=0\\\frac{\partial p}{\partial x}=0\\\frac{\partial T}{\partial x}=0\end{array}\right\} \qquad (13)$$

3 Wall boundary

The velocity on the wall equal to zero

$u=v=0$

The first derivative of pressure in the direction normal to the wall equal to zero

$$\frac{\partial p}{\partial y}=0 \qquad (14)$$

For constant heat flux on bottom plane

$$T_w = q * \frac{y}{k} + T_{ij} \tag{15}$$

And for adiabatic for top plate

$$\frac{\partial T}{\partial y} = 0 \tag{16}$$

Heat transfer and pressure drop calculations

The aim of present numerical study is to know logically the effect of triangle protrusion on local heat transfer and pressure drop by calculation Nusselt number (Nu) and pressure coefficient (C_p) as follows.

1 Heat transfer calculation

To calculate Nusselt number (Nu) from heated wall at constant heat flux, first the temperature distribution can be calculated from the following equation.

$$q_{wall} = -k \frac{\partial T}{\partial n} \tag{17}$$

Where n is the normal distance

Then calculate local Nusselt number (Nu_{ij}) as follows:-

$$q_{wall}=q_{conv} \tag{18}$$

$$q_{wall}=h_{(ij)}*(T_{(ij)}-T_b) \tag{19}$$

$$Nu_{(ij)}=h_{(ij)}*H/k_f \tag{20}$$

2 Local static pressure coefficient

The Local static pressure coefficient along the wall surface can be calculated as follows:-

$$cp_{(ij)}=\frac{(p_{(ij)} - p_o)}{0.5 \rho u_{in}^2} \tag{21}$$

Results and discussion

A number of computations have been performed at different (d/H) for protrusion. **Figure (6)** shows the stream lines for the flow in channel without using protrusion (free case). There is no change in direction of stream and no vortex appears.

Figure (7) shows the stream lines for the flow in channel with using triangular protrusion with different (d/H). When (d/H) be a large value, the effect of protrusion is nearly equal to free case but when it be small, the procedure of velocity vectors will be changing when the flow reaches the protrusion and the direction of velocity will be changing toward the main flow, and due to the high momentum of the main flow in the middle of channel, the velocity will be change its direction behind the protrusion as in **Figures (a, b).** At small (d/H) the vortex will be appearing behind the protrusion because pressure different across the protrusions as in **Figures (c, d, e and f).**

Figure (8) shows the temperature contours for flow inside channel without using protrusion, the temperature gradient due to the thermal resistance (thermal boundary layer) clearly appeared, the thermal resistance at entrance of channel is equal to zero and it increases toward the rear due to the growth thermal boundary layer.

Figure (9) shows the temperature contours for flow inside channel with using protrusion with different (d/H), the temperature gradient is different from the free case because of destroy the thermal boundary layer, also the figures shows that the heat transfer will be increasing in front of protrusion due to sweeping the heat toward the main flow but it be decreasing behind the protrusion.

Figure (10) shows the pressure coefficient at different protrusion base along the channel. The figure shows that when the protrusion base be small [(d/H) be small], the pressure drops will be increasing near the position of protrusion since the different across the faces of protrusion and it will be decrease when increasing (d/H). Maximum local pressure drop occur was at d/H=0.

Figure (11) shows the Nusselt number distribution along the plate surface for free case and with using triangle protrusion with different (d/H), the figure shows that the local heat transfer before the protrusion position for all cases are equal and its will be changing when the flow reaches the protrusion, heat transfer will be increasing at the front face of protrusion because of the flow will be sweeping the heat at this region and Nusselt number reaches maximum value at the tip of protrusion. At the rear face of protrusion, heat transfer will be increasing slightly because of the vortex of flow will be appearing in the rear of protrusion specially at small (d/H) and the effect of the triangle protrusion will be continuing to the rear of plate. Maximum local heat transfer occurs at d/H=0.26.

Figure (12) shows the comparison of local Nusselt number for free case between the present study and reference (Ahmed, 2003) at the same conditions, the figure shows that the same procedure in two carves.

Conclusions

Local heat transfer and pressure drop of plate fins with using protrusions have been measured and compared with free case. The most important results can be summarized as follows:-

- Protrusion accelerate the flow to sweep the heat from high heated region in plates, also it's mixing the hot fluid near the wall with the cold fluid at the main flow.
- Average heat transfer enhanced (6% -21%) when using Protrusion with different ratio of (d/H).
- Maximum average heat transfer enhanced when using Protrusion with (d/H= 0.26).
- Pressure drop more than free case when using Protrusion and average pressure drop increased (2% -16%) with using Protrusions with different ratio of (d/H)..
- Pressure drop increases when decrease d/H.

References

1- Ahmed, S. and Lars, D. "Numerical study of heat and flow in plate- fin heat exchanger with vortex generators " *Turbulence heat and mass transfer4*, pp 1155-1162, 2003.

2- Ahmed, H. Jallal, J and Hassan, K. "*Enhancement heat transfer from heated cylinder inside duct by using vortex generators*" PhD thesis, Mechanical Engineering Department University of Technology, Iraq, 2006.

3- Biswas, G. and Chattapdhyay, H "Heat transfer in channel with built - in wing type- vortex generators " *Int. J. heat mass transfer* vol.15, No.4, pp 803-814, 1992.

4- Fiebig, M. Brockmeier, U. Mitra, N. and Guntermann, T "Structure of velocity and temperature fields in laminar channel flow with longitudinal vortex generators " *Numerical heat transfer*, Part A, Vol.15, pp 281-302, 1989.

5- Ferzigen, J. and Peric, M. "*Computational method for fluid dynamic*" 2-th edition Springer, Berlin, 1999.

6- Isak, K. Teoman, A. Hayati, O. and Betiil, A. "Heat transfer and flow structure in rectangular channel with winglet type vortex generators " *Tr. J. of Engineering and Environmental Science*, vol.22, pp 185-195, 1998.

7- Patenker, S. V. "Numerical heat transfer and fluid flow. Hemispere Publishing Mc Graw-hill Book co. 1980.

8- Russell, C. Jones, T. and Lee, G. "heat transfer enhancement using vortex generators " *Seventh int. heat transfer conf*. Munich, Federal Republic of Germany, pp 283-288, 1982.

9- Tiggelbeek, S. Mitra, N. and Fiebig, M. "Comparison of wing type vortex generators for heat transfer enhancement in channel flows " *ASME*, vol. 116, pp 880-885, 1991.

10- Thompson, J. F. Thomas, F. C. and Mastin "TOMACA-A code for numerical generation of boundary - fitted curvilinear coordinate system on field containing any number or arbitrary 2 -D bodies " J of computational physics, vol/24, pp 274-303, 1977.

11- Yunliang, W. and Satoru, K. "Production of duct flows with a pressure- based procedure " *Numerical heat transfer*, Part A, vol/33, pp 723-748, 1998.

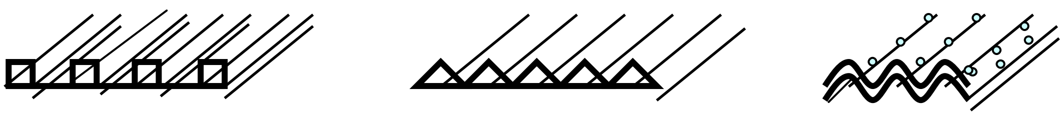

(a) (b) (c)

Figure (1) surface geometries for plat- fin heat exchanger (a) plain Rectangular fins, (b) plain triangular fins, (c) perforated fins

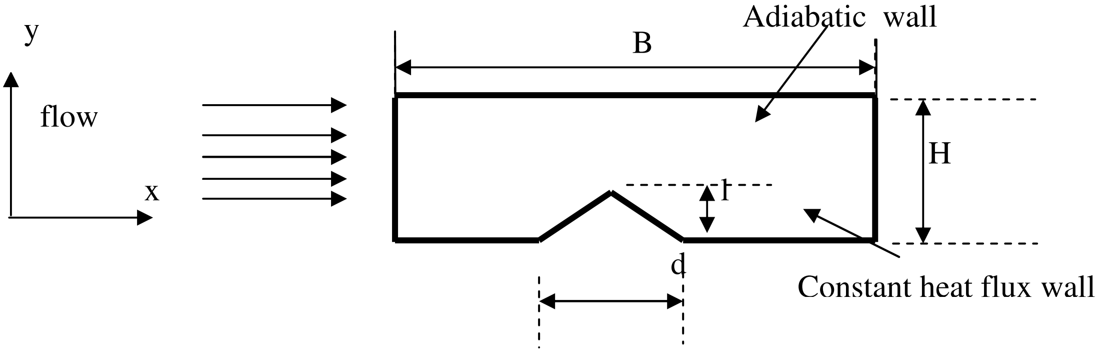

Figure (2) proposed flow domain

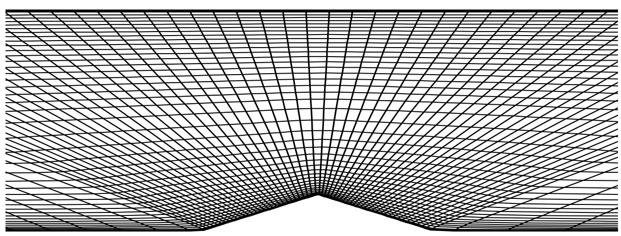

Figure (3) grid generated

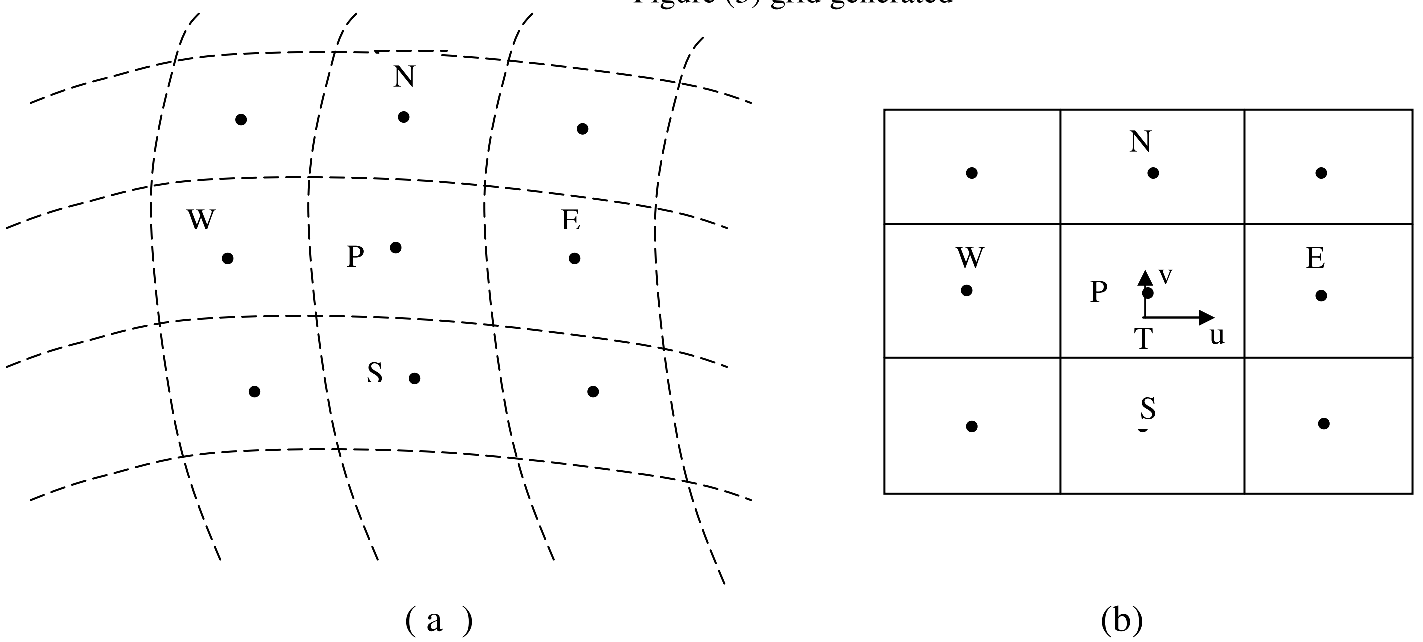

Figure (4) (a) Physical Plane (x,y) (b)Computational Plane (ξ,η)

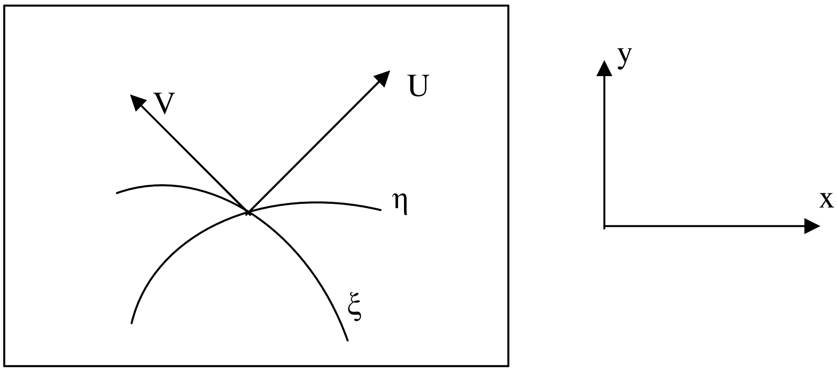

Figure (5) the contravariant velocity components

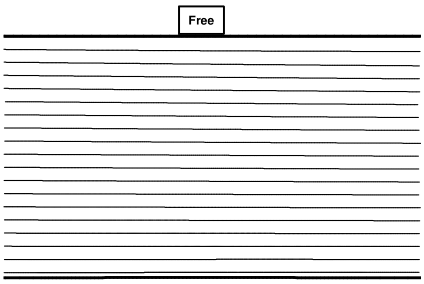

Figure (6) Stream lines for free case

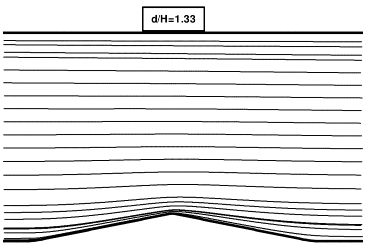

(a)

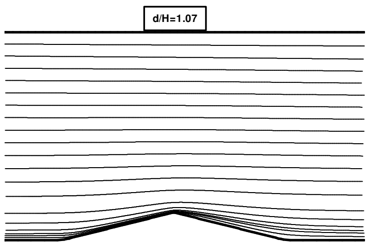

(b)

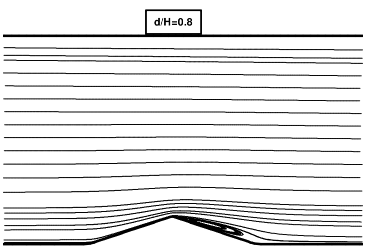

(c)

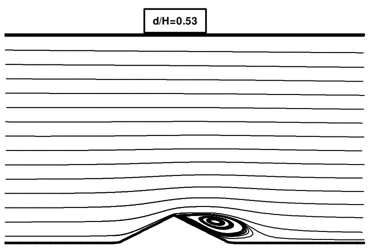

(d)

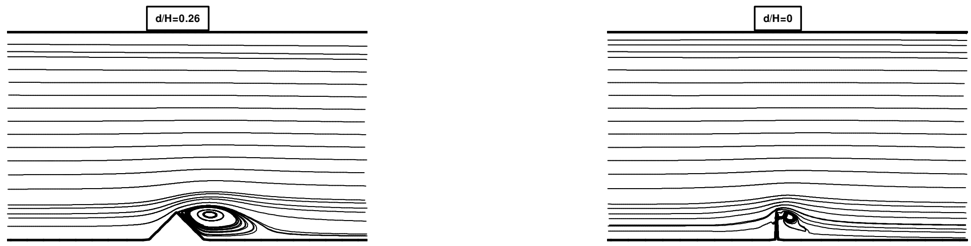

(e) (f)

Figure (7) stream line distribution (a) d/H=1.33, (b) d/H=1.07 (c) d/H=0.8, (d) d/H=0.53, (e) d/H=0.26, (f) d/H=0

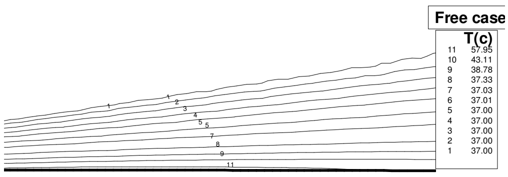

Figure (8) Temperature contour for free case

(b) (a)

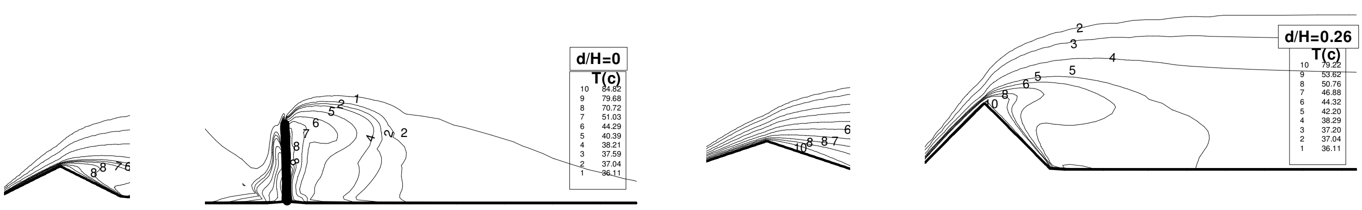

Figure (9) Temperature counters (a) d/H=1.33, (b) d/H=1.07 (c) d/H=0.8, (d) d/H=0.53, (e) d/H=0.26, (f) d/H=0

(f) (e)

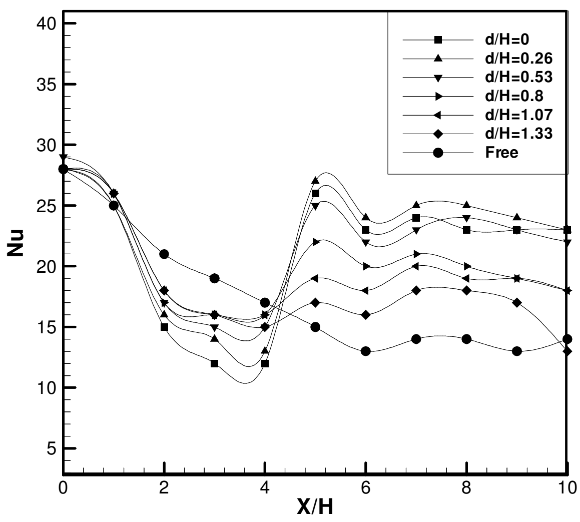

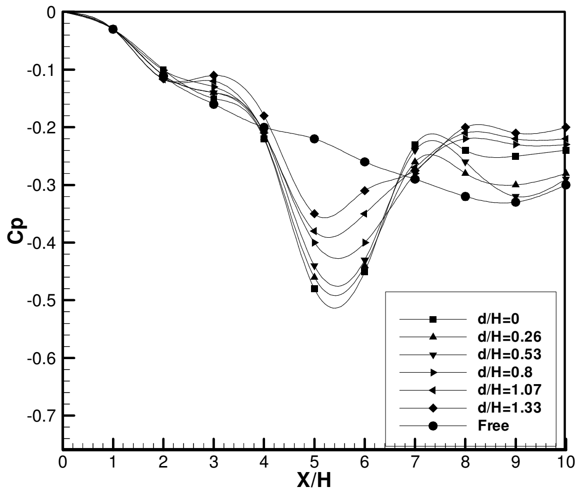

Figure (10) pressure coefficient distribution Figure (11) Nusselt number distribution

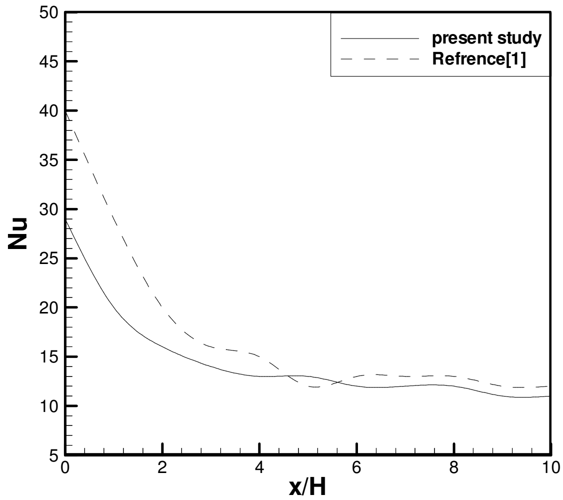

Figure (12) Comparison of Nusselt number with reference [1]